T Cell Requirement for Development of Chronic Ulcerative Dermatitis in E- and P-Selectin-Deficient Mice[1]

S. Bradley Forlow,*† E. James White,* Kennard L. Thomas,*§ Gregory J. Bagby,¶ Patricia L. Foley,‡ and Klaus Ley[2]*†

C57BL/6 mice deficient in E- and P-selectin ($E^{-/-}P^{-/-}$) kept under specific pathogen-free barrier conditions have high circulating neutrophil counts and develop hypercellular cervical lymph nodes with substantial plasma cell infiltrates, severe ulcerative dermatitis, conjunctivitis, and lung pathology, which eventually lead to premature death. To test the hypothesis that the pathology in $E^{-/-}P^{-/-}$ mice may be caused by dysfunctional lymphocyte activity, we crossed $E^{-/-}P^{-/-}$ mice with recombination activation gene (Rag)-$1^{-/-}$ mice to generate $E^{-/-}P^{-/-}$Rag-$1^{-/-}$ mice lacking mature T and B lymphocytes. $E^{-/-}P^{-/-}$Rag-$1^{-/-}$ mice had circulating neutrophil counts and plasma G-CSF levels similar to $E^{-/-}P^{-/-}$ mice. Remarkably, none of the $E^{-/-}P^{-/-}$Rag-$1^{-/-}$ mice developed conjunctivitis or ulcerative dermatitis typical of $E^{-/-}P^{-/-}$ mice. These mice were overall healthier in appearance than $E^{-/-}P^{-/-}$ mice, and histopathologic changes in the lung were reduced. Cervical lymph nodes in $E^{-/-}P^{-/-}$Rag-$1^{-/-}$ mice were much smaller than those of $E^{-/-}P^{-/-}$ mice, containing few mononuclear cells and no plasma cells. These data show that the severe disease phenotype of $E^{-/-}P^{-/-}$ mice depends on lymphocyte function. We conclude that a dysregulated immune response in $E^{-/-}P^{-/-}$ mice causes disease development, but is not necessary for elevated neutrophil counts. ***The Journal of Immunology,*** **2002, 169: 4797–4804.**

Leukocyte adhesion molecule-deficient mice have been used extensively to elucidate the molecular mechanisms of leukocyte recruitment. Although mice lacking P-selectin ($P^{-/-}$), E-selectin ($E^{-/-}$), L-selectin ($L^{-/-}$), or ICAM-1 (ICAM-$1^{-/-}$) have defective neutrophil recruitment in some inflammatory models, these mice do not show a distinctive spontaneous phenotype and have normal viability. Mice lacking CD18 integrins ($CD18^{-/-}$) and mice lacking both E- and P-selectin ($E^{-/-}P^{-/-}$) display a dramatic reduction in neutrophil recruitment in some inflammatory models (1–5). $CD18^{-/-}$ and $E^{-/-}P^{-/-}$ mice develop a severe phenotype characterized by facial and submandibular ulcerative dermatitis (1, 4). The development of skin lesions in $E^{-/-}P^{-/-}$ mice occurs at variable ages after weaning with >90% of the mice showing lesions by 6–8 mo (1, 4, 6). Histopathological analysis of the affected skin showed a loss of the overlying squamous epithelium and superficial colonization by bacteria (1). Cultures on afflicted skin were positive for common bacterial flora, including *Staphylococcus aureus*, *Escherichia coli*, *Enterococcus faecium*, *Staphylococcus xylosus*, and *Staphylococcus viridans* (1, 4). Cultures for bacterial and fungal organisms have been consistently negative in the blood, spleen, liver, lymph nodes, and lungs of these mice, suggesting that bacterial colonization of skin lesions is secondary to skin ulceration (1, 4). The causative factors leading to the development of ulcerative dermatitis have not been identified.

Mice lacking E-, P-, and L-selectin ($E^{-/-}P^{-/-}L^{-/-}$) have been generated by two groups. Robinson et al. (7) reported that the $E^{-/-}P^{-/-}L^{-/-}$ mice (Hynes mutation) developed ulcerative dermatitis although the frequency and age of onset were not evaluated. The $E^{-/-}P^{-/-}L^{-/-}$ mice described by Collins et al. (8) (Baylor mutation) are largely protected from ulcerative dermatitis seen in $E^{-/-}P^{-/-}$ mice. Only 3 of 156 $E^{-/-}P^{-/-}L^{-/-}$ mice showed ulcerative dermatitis by 6 mo of age (8). However, this same line of $E^{-/-}P^{-/-}L^{-/-}$ mice (Baylor mutation) developed skin lesions at another facility (University of Washington, Seattle, WA), suggesting that lesion development is related to differences in animal husbandry and environment. Mice deficient in E- and P-selectin and ICAM-1 ($E^{-/-}P^{-/-}I^{-/-}$) show a complete protection from the development of ulcerative dermatitis (9), suggesting a role for ICAM-1 in the development of ulcerative dermatitis that occurs in the absence of E- and P-selectin.

The relative protection from ulcerative dermatitis in $E^{-/-}P^{-/-}L^{-/-}$ and $E^{-/-}P^{-/-}I^{-/-}$ mice suggests that both L-selectin and ICAM-1 may serve a function critical to lesion development. L-selectin is necessary for lymphocyte homing into peripheral lymph nodes (10) and for lymphocyte recirculation (11). As a result, L-selectin-deficient mice have altered lymphocyte function, impaired T cell responses, and display very small lymph nodes (12). Because trafficking of naive lymphocytes is impaired in $E^{-/-}P^{-/-}L^{-/-}$ mice, the immune response to bacterial Ags present in the normal flora may be reduced. T cell-stimulating activity was also shown to be impaired in mice lacking ICAM-1, suggesting that ICAM-1 is an important costimulatory molecule (13). Based on these findings, we hypothesized that defective lymphocyte function in $E^{-/-}P^{-/-}L^{-/-}$ and $E^{-/-}P^{-/-}I^{-/-}$ mice protects these mice from lesion development. We inferred that the ulcerative dermatitis seen in $E^{-/-}P^{-/-}$ mice may be lymphocyte-dependent. To test the hypothesis that the development of ulcerative dermatitis in $E^{-/-}P^{-/-}$ mice requires mature T cells, we generated mice deficient in E- and P-selectin and the V(D)J

*Department of Biomedical Engineering, †Cardiovascular Research Center, and ‡Center for Comparative Medicine, University of Virginia, Charlottesville, VA 22908; §Center for Blood Research, Harvard Medical School, Boston, MA 02115; and ¶Department of Physiology, Louisiana State University Health Sciences Center, New Orleans, LA 70112

Received for publication June 4, 2002. Accepted for publication August 29, 2002.

The costs of publication of this article were defrayed in part by the payment of page charges. This article must therefore be hereby marked *advertisement* in accordance with 18 U.S.C. Section 1734 solely to indicate this fact.

[1] This work was supported by National Institutes of Health Grants HL54136 (to K.L.) and NRSA-HL10447 (to S.B.F.).

[2] Address correspondence and reprint requests to Dr. Klaus Ley, Cardiovascular Research Center, University of Virginia, Health System Box 801394, Charlottesville, VA 22908. E-mail address: klausley@virginia.edu

0022-1767/02/$02.00

recombination activation gene (Rag)[3]-1 (14) ($E^{-/-}P^{-/-}$Rag-$1^{-/-}$) by cross-breeding $E^{-/-}P^{-/-}$ with Rag-$1^{-/-}$ mice. Mice lacking the V(D)J Rag-1 do not have mature T or B lymphocytes (14). $E^{-/-}P^{-/-}$Rag-$1^{-/-}$ mice are healthier than $E^{-/-}P^{-/-}$ mice and do not develop ulcerative dermatitis seen in $E^{-/-}P^{-/-}$ mice.

Materials and Methods

Mice

Mice deficient in both E- and P-selectin and Rag-1 were generated by cross-breeding $E^{-/-}P^{-/-}$ C57BL/6 N6 (1) and Rag-$1^{-/-}$ C57BL/6 N10 (The Jackson Laboratory, Bar Harbor, ME) mutants. F_1 hybrids were back-crossed to $E^{-/-}P^{-/-}$ to generate $E^{+/-}P^{+/-}$Rag-1^{+} and $E^{-/-}P^{-/-}$Rag-1^{+} mice. F_1 hybrids were back-crossed to Rag-$1^{-/-}$ mice to generate $E^{+/+}P^{+/+}$Rag-$1^{-/-}$ and $E^{+/-}P^{+/-}$Rag-$1^{-/-}$. Breedings were established from these offspring to generate all necessary control groups, including $E^{+/+}P^{+/+}$Rag-1^{+}, $E^{+/-}P^{+/-}$Rag-1^{+}, $E^{+/+}P^{+/+}$Rag-$1^{-/-}$, $E^{+/-}P^{+/-}$Rag-$1^{-/-}$, $E^{-/-}P^{-/-}$Rag-1^{+}, and $E^{-/-}P^{-/-}$Rag-$1^{-/-}$ mice. Because there is no evidence for haplo-insufficiency in any of the selectin mutants, $E^{+/-}P^{+/-}$ mice were pooled with $E^{+/+}P^{+/+}$ mice. Wild-type refers to $E^{+/+}P^{+/+}$Rag-1^{+} and $E^{+/-}P^{+/-}$Rag-1^{+} mice; Rag-$1^{-/-}$ refers to $E^{+/+}P^{+/+}$Rag-$1^{-/-}$ and $E^{+/-}P^{+/-}$Rag-$1^{-/-}$ mice; and $E^{-/-}P^{-/-}$ refers to $E^{-/-}P^{-/-}$Rag-1^{+} mice.

Polymerase chain reaction

Genomic DNA was analyzed using PCR for the wild-type and knockout E- and P-selectin alleles. The P-selectin PCR assay used a forward primer from exon 3 of murine P-selectin (5′-TCA CGG GTG TTC TGT AGG AGG-3′) and a reverse primer from exon 3 (5′-GGG GCC GAG TTA CTC TTG ATG-3′), yielding a 260-bp wild-type fragment. The P-selectin knockout allele was detected using a forward primer from exon 2 (5′-GCT GGC TGC CCA AAA GGT T-3′) and a reverse primer from the inserted neomycin resistance gene (5′-ACC CGT GAT ATT GCT GAA GAG C-3′). This reaction yielded a 1300-bp mutant fragment. PCR conditions for the detection of the wild-type alleles were 94°C for 4 min, 35 cycles of 94°C for 30 s, 55°C for 30 s, and 72°C for 30 s, followed by 72°C for 7 min. PCR conditions for the detection of the P-selectin knockout alleles were 94°C for 4 min, 35 cycles of 94°C for 1 min, 61°C for 1 min, and 72°C for 1 min, followed by 72°C for 7 min.

The E-selectin PCR assay used a forward primer from exon 5 of murine E-selectin (5′-TTG GCT GTA AAA GGG GCT ACC-3′) and a reverse primer from exon 6 (5′-CAT GAT GGC GTC TCG TTA TCC-3′), yielding a 1000-bp wild-type fragment. The E-selectin knockout allele was detected by a forward primer from hypoxanthine phosphoribosyltransferase gene (5′-ACT ATC AGT TCC CTT TGG GCG-3′) and the reverse primer (5′-CAT GAT GGC GTC TCG TTA TCC-3′), which yields a 650-bp knockout fragment. PCR conditions for the detection of the E-selectin wild-type alleles were 94°C for 4 min, 35 cycles of 94°C for 1 min, 57°C for 1 min, and 72°C for 1 min, followed by 72°C for 7 min. PCR conditions for the detection of the E-selectin knockout allele were 94°C for 4 min, 35 cycles of 94°C for 1 min, 59°C for 1 min, and 72°C for 1 min, followed by 72°C for 7 min.

Serum G-CSF measurements

Serum G-CSF protein concentrations were determined using a specific enzyme-linked immunoassay using Ab pairs purchased from R&D Systems (Minneapolis, MN). For this purpose, 96-well plates (NuncImmunoplate Maxisorb; Nunc, Neptune, NJ) were coated with 2 μg/ml of capture Ab and incubated overnight at 4°C. The plates were then washed five times with wash buffer (0.05% Tween 20 in PBS) and blocked with 200 μl 2% BSA in wash buffer for 2 h at room temperature. G-CSF standards and samples were diluted in wash buffer containing 2% FCS. Both standards (31.25–1000 pg/ml) and samples (50 μl) were added to wells and the plates were incubated for 1 h at 37°C. After washing, 50 μl of biotinylated anti-G-CSF (0.1 μg/ml in dilution buffer) was added and the plates were incubated for 1 h at 37°C. Wells were then washed and incubated for 1 h after adding 100 μl of 0.1 μg/ml peroxidase-conjugated streptavidin (Jackson ImmunoResearch Laboratories, West Grove, PA) in dilution buffer. After washing the plate, 100 μl of tetramethylbenzidine (Sigma-Aldrich, St. Louis, MO) was added as substrate and color was allowed to develop for 30 min in the dark. After stopping the reaction with 50 μl of 3 M H_2SO_4, ODs were determined at 450 nm. G-CSF concentrations were calculated from the standard curve using log-log linear regression.

Flow cytometry

Peripheral blood was collected from the tail vein. Expression of CD4 and CD8 on peripheral lymphocytes was determined by direct immunofluorescence to identify mice lacking the V(D)J Rag-1. Lymphocytes were identified and gated by forward and side scatter properties. $CD8^+$ cells were identified by FITC-labeled mAb 53-6.7 (BD PharMingen, San Diego, CA) staining. $CD4^+$ cells were identified by FITC-labeled mAb GK1.5 (BD PharMingen) staining. Cells were analyzed by forward scatter, side scatter, and FITC fluorescence using a laser flow cytometer (FACSCan; BD Biosciences, Mountain View, CA). Data are presented as fluorescence histograms of CD4 and CD8 expression on a four-decade log scale.

Histopathology

Age-matched wild-type, Rag-$1^{-/-}$, $E^{-/-}P^{-/-}$ with and without ulcerative dermatitis, and $E^{-/-}P^{-/-}$Rag-$1^{-/-}$ mice were euthanized by cervical dislocation under anesthesia for histopathological analysis. After gross examination for any discernable pathology, lung, intestine, kidney, cervical lymph nodes, liver, spleen, and skin samples were fixed in 10% buffered formalin (Sigma-Aldrich), embedded in paraffin, sectioned, and examined after H&E staining.

Microbiological analyses

Tissue samples for microbiologic analysis were obtained under sterile conditions from the lung, liver, and spleen from wild-type Rag-$1^{-/-}$, $E^{-/-}P^{-/-}$ with and without ulcerative dermatitis, and $E^{-/-}P^{-/-}$Rag-$1^{-/-}$ mice. Tissues were homogenized with a sterile grinder in 0.5 ml PBS. A 100-μl sample from each tissue was plated onto trypticase soy agar with 5% sheep RBCs (Difco, Detroit, MI). Plates were observed at 24 and 48 h for growth.

Statistics

Total leukocyte counts, neutrophil counts, mononuclear cell counts, and serum G-CSF levels between groups were compared using Kruskal-Wallis One-Way ANOVA on ranks and pairwise multiple comparison by Dunn's method. Spleen weights and lymph node weights between groups were compared using Kruskal-Wallis one-way ANOVA and pairwise multiple comparison by the Tukey test. Statistical significance was set at $p < 0.05$.

Results

Generation of $E^{-/-}P^{-/-}$Rag-$1^{-/-}$ mice

Mice deficient in E- and P-selectin and Rag-1 were generated by cross-breeding $E^{-/-}P^{-/-}$ C57BL/6 N6 (1) and Rag-$1^{-/-}$ C57BL/6 N10 (The Jackson Laboratory) mutants. This resulted in all necessary control groups, including $E^{+/+}P^{+/+}$Rag-1^{+} (wild-type), $E^{+/-}P^{+/-}$Rag-$1^{-/-}$ (Rag-$1^{-/-}$), $E^{-/-}P^{-/-}$Rag-$1^{+/+}$ ($E^{-/-}P^{-/-}$), and $E^{-/-}P^{-/-}$Rag-$1^{-/-}$ (Fig. 1*A*; Table I). Mice expressing E- and P-selectin ($E^{+/+}P^{+/+}$), heterozygous for E- and P-selectin ($E^{+/-}P^{+/-}$), and homozygous for a null mutation in E- and P-selectin ($E^{-/-}P^{-/-}$) were determined by PCR. Consistent with previous results (1, 4) and the close distance of the E- and P-selectin genes, we found that E- and P-selectin cosegregated in all mice tested.

Mice expressing E- and P-selectin ($E^{+/+}P^{+/+}$) show a band from the wild-type P-selectin reaction at 260 bp and at 1000 bp from the E-selectin wild-type reaction (Fig. 1*A*, *lane 1*). No band is detectable from either of the knockout reactions in $E^{+/+}P^{+/+}$ mice (Fig. 1*A*, *lane 2*). A heterozygous mutation for E- and P-selectin ($E^{+/-}P^{+/-}$) results in both wild-type and knockout bands from the P-selectin and the E-selectin reactions (Fig. 1*A*, *lanes 3* and *4*). Mice that have a null mutation in E- and P-selectin ($E^{-/-}P^{-/-}$) show no band from either wild-type reaction (Fig. 1*A*, *lanes 5* and *7*) and a single band from the respective knockout reactions (Fig. 1*A*, *lanes 6* and *8*). Verification for a null mutation for Rag-1 was determined by flow cytometry. Mice deficient in Rag-1 have no $CD4^+$ or $CD8^+$ lymphocytes in blood (Fig. 1*B*, *bottom panels*).

[3] Abbreviations used in this paper: Rag, recombination activation gene.

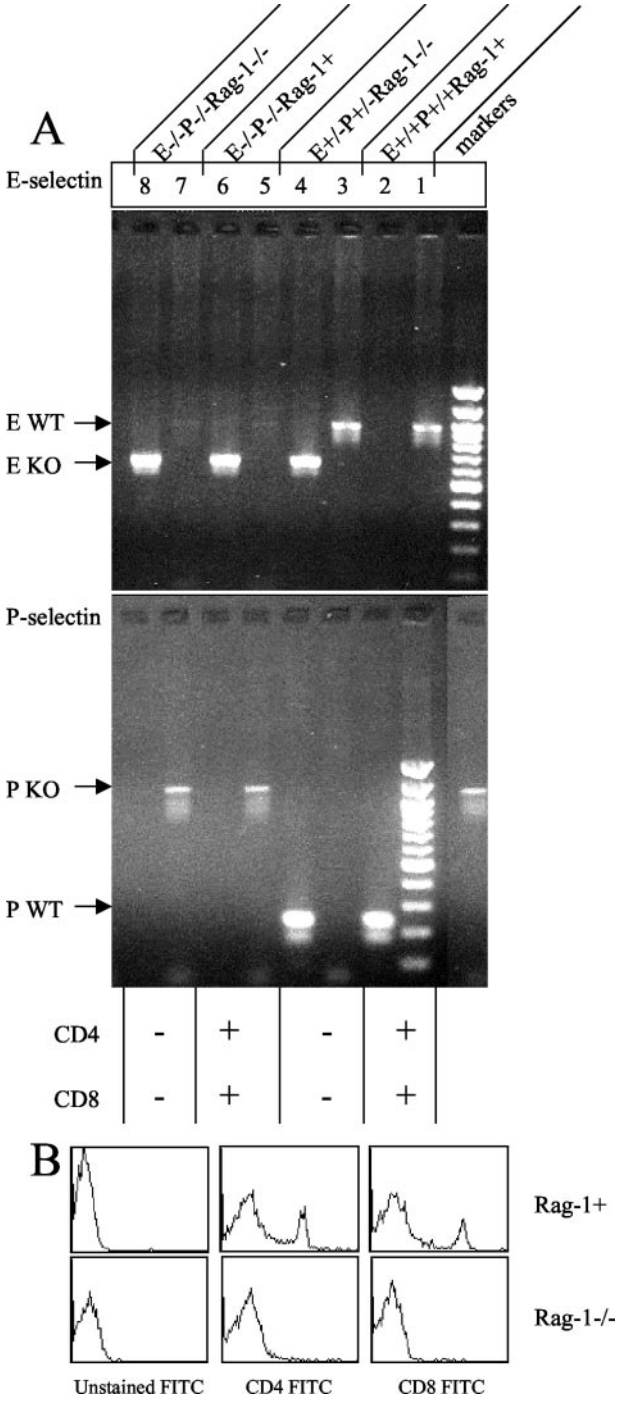

FIGURE 1. $E^{-/-}P^{-/-}$Rag-$1^{-/-}$ mice were identified by PCR and flow cytometry. *A*, PCR was used to determine mice expressing E- and P-selectin ($E^{+/+}P^{+/+}$), heterozygous for E- and P-selectin ($E^{+/-}P^{+/-}$), and homozygous null mutations in E- and P-selectin ($E^{-/-}P^{-/-}$). The E-selectin genotype was identified by a 650-kb mutant fragment and a 1000-kb wild-type fragment. The P-selectin genotype was identified by a 1300-kb mutant fragment and a 260-kb wild-type (WT) fragment. *B*, Rag-1-deficient mice were identified by absence of $CD4^+$ and $CD8^+$ expressing cells in whole blood using flow cytometry. KO, Knockout.

White blood cell counts and serum G-CSF levels

Because mice deficient in Rag-1 do not develop functional T or B lymphocytes, Rag-$1^{-/-}$ mice show a significant reduction of mononuclear cells in the peripheral circulation compared with wild-type mice (Table II). Rag1-deficient mice had neutrophil counts similar to wild-type mice (Table II). $E^{-/-}P^{-/-}$ mice displayed significantly elevated leukocyte counts compared with wild-type and Rag-$1^{-/-}$ mice. $E^{-/-}P^{-/-}$ mice were severely neutrophilic (Table II). Neutrophil counts in $E^{-/-}P^{-/-}$Rag-$1^{-/-}$ mice were almost as high as in $E^{-/-}P^{-/-}$ mice. However, $E^{-/-}P^{-/-}$Rag-$1^{-/-}$ mice had significantly fewer circulating mononuclear cells than $E^{-/-}P^{-/-}$ mice (Table II).

Table I. *No. of mice in study*

	No. of Mice
Wild type	67
Rag-$1^{-/-}$	33
$E^{-/-}P^{-/-}$	35
$E^{-/-}P^{-/-}$Rag-$1^{-/-}$	62

Consistent with elevated circulating neutrophil levels, $E^{-/-}P^{-/-}$ mice showed increased serum G-CSF levels compared with wild-type and Rag-$1^{-/-}$ mice (Table II). $E^{-/-}P^{-/-}$Rag-$1^{-/-}$ mice showed G-CSF levels similar to $E^{-/-}P^{-/-}$ mice (Table II). Similar increases in neutrophil counts and G-CSF levels in $E^{-/-}P^{-/-}$Rag-$1^{-/-}$ mice compared with $E^{-/-}P^{-/-}$ mice show that the level of neutrophilia in these mice is not dependent on lymphocyte function (Table II).

Clinical and pathological findings

$E^{-/-}P^{-/-}$Rag-$1^{-/-}$ mice were generally healthier than $E^{-/-}P^{-/-}$ mice. $E^{-/-}P^{-/-}$Rag-$1^{-/-}$ breeders consistently produced litters for ~1 year. $E^{-/-}P^{-/-}$ breeders only occasionally generated litters until 5–6 mo of age in the same specific pathogen-free barrier facility. Therefore, the $E^{-/-}P^{-/-}$ colony was maintained with heterozygous breeders.

Approximately 50% (18 of 35) of the $E^{-/-}P^{-/-}$ mice 6–12 mo old developed conjunctivitis and/or facial and submandibular ulcerative dermatitis (Fig. 2*C*). Initially, these mice showed hair loss around the eyes and the development of conjunctivitis. This was followed by hair loss on the nose and neck and subsequent skin lesion development (Fig. 2*A*). These lesions have primarily been shown to be colonized by commensal bacteria, but not specific pathogens (1, 4). $E^{-/-}P^{-/-}$Rag-$1^{-/-}$ mice were completely protected from the development of ulcerative dermatitis (Fig. 2*B*). None of the 62 $E^{-/-}P^{-/-}$Rag-$1^{-/-}$ mice developed facial or submandibular ulcerative dermatitis, including 25 mice older than 12 mo (Fig. 2*C*).

Microbiological cultures

To investigate possible bacteremia and colonization of internal organs by commensal bacteria in $E^{-/-}P^{-/-}$ mice, liver, lung, and spleen samples were analyzed for bacterial growth. No positive cultures were obtained in wild-type ($n = 4$), Rag-$1^{-/-}$ ($n = 5$), $E^{-/-}P^{-/-}$ showing ulcerative dermatitis ($n = 5$), $E^{-/-}P^{-/-}$ with no signs of ulcerative dermatitis ($n = 5$), or $E^{-/-}P^{-/-}$Rag-$1^{-/-}$ ($n = 8$) mice.

Histopathology

Cervical skin from $E^{-/-}P^{-/-}$Rag-$1^{-/-}$ mice showed an intact epidermis, no dermal infiltrate, and no bacterial colonization (Fig. 3*C*). Tissue samples from $E^{-/-}P^{-/-}$ mice with ulcerative skin lesions showed areas of epidermal loss as well as hyperplastic epithelium, and a dermal infiltrate consisting of mixed inflamma-

Table II. *Leukocyte counts and serum G-CSF levels*[a]

	Total Leukocyte Counts (cells/μl)	Neutrophils/μl	Mononuclear Cells/μl	Serum G-CSF (pg/ml)
Wild type	15,000 ± 1,000	2,000 ± 200	12,000 ± 1,000	24 ± 4
Rag-1$^{-/-}$	3,500 ± 300[b]	1,700 ± 200	3,000 ± 600[e]	43 ± 6
E$^{-/-}$P$^{-/-}$	41,000 ± 2,000[c]	23,000 ± 1,000[c]	18,000 ± 1,000[f]	72 ± 11[g]
E$^{-/-}$P$^{-/-}$Rag-1$^{-/-}$	22,000 ± 2,000[d]	18,000 ± 1,000[c]	4,100 ± 300[f]	91 ± 16[g]

[a] All values expressed as mean ± SEM.
[b] Different from all other groups.
[c] Different from wild-type and Rag-1$^{-/-}$ groups.
[d] Different from Rag-1$^{-/-}$ group.
[e] Different from wild-type and E$^{-/-}$P$^{-/-}$ groups.
[f] Different from Rag-1$^{-/-}$ and E$^{-/-}$P$^{-/-}$Rag-1$^{-/-}$ groups.
[g] Different from wild-type group ($p < 0.05$).

tory cells, including mast cells, macrophages, and mononuclear cells (Fig. 3, *A* and *B*). Areas of ulceration also contained large numbers of bacterial colonies both on the denuded surface and infiltrating the underlying dermis (Fig. 3*B*). Neutrophils were noticeably lacking despite extensive bacterial colonization. There was also evidence of loss of sebaceous glands and distortion of hair follicles.

The splenic architecture of wild-type mice showed normal, well-defined regions of red and white pulp (Fig. 4). As expected, the lymphoid follicles (white pulp) were absent in Rag-1$^{-/-}$ mice (Fig. 4), but some myeloid and erythroid precursor cells were present. E$^{-/-}$P$^{-/-}$ mice showed a profound expansion of red pulp due to extramedullary hemopoiesis, disrupting the normal splenic architecture (Fig. 4). Large numbers of megakaryocytes, erythroid, myeloid precursors, neutrophils, and plasma cells were present throughout the spleen. The white pulp in these mice was smaller, distorted, and less distinct (Fig. 4). E$^{-/-}$P$^{-/-}$Rag-1$^{-/-}$ mice exhibited a similar pattern of extramedullary hemopoiesis; however, these mice showed an absence of white pulp (Fig. 4). As a result of extramedullary hemopoiesis, the spleen weights normalized for body weights in E$^{-/-}$P$^{-/-}$ and E$^{-/-}$P$^{-/-}$Rag-1$^{-/-}$ mice were increased ~3- and 2-fold, respectively, compared with wild-type and Rag-1$^{-/-}$ mice (Table III).

Lung sections from Rag-1$^{-/-}$ mice (Fig. 5) were indistinguishable from wild-type mice (data not shown). Mice lacking E- and P-selectin showed degrees of lung pathology varying from mild to severe. Interstitial cellularity was increased secondary to leukocyte infiltration (Fig. 5), and in more severe cases evidence of interstitial edema and hemorrhage were present. E$^{-/-}$P$^{-/-}$Rag-1$^{-/-}$ mice generally had less inflammatory cell infiltrate in the lungs compared with E$^{-/-}$P$^{-/-}$ mice (Fig. 5). Where seen, infiltrates appeared to be more focal than diffusely distributed.

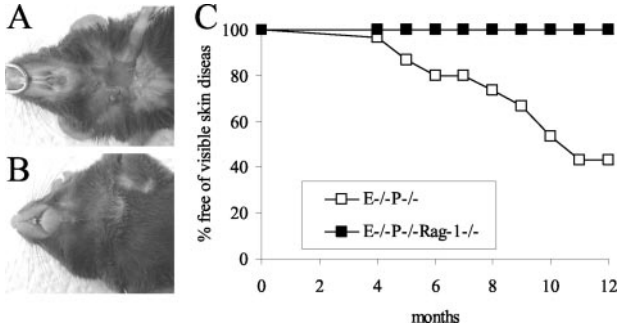

FIGURE 2. E$^{-/-}$P$^{-/-}$Rag-1$^{-/-}$ mice do not develop ulcerative dermatitis. *A*, Mice lacking E- and P-selectin often develop conjunctivitis that progresses to ulcerative dermatitis on the nose and neck. *C*, Approximately 50% of E$^{-/-}$P$^{-/-}$ mice displayed ulcerative dermatitis or conjunctivitis by 10 mo of age. *B*, E$^{-/-}$P$^{-/-}$Rag-1$^{-/-}$ mice are protected from the development of ulcerative dermatitis. None of the 62 E$^{-/-}$P$^{-/-}$Rag-1$^{-/-}$ mice developed lesions, including 25 mice >12 mo old (*C*).

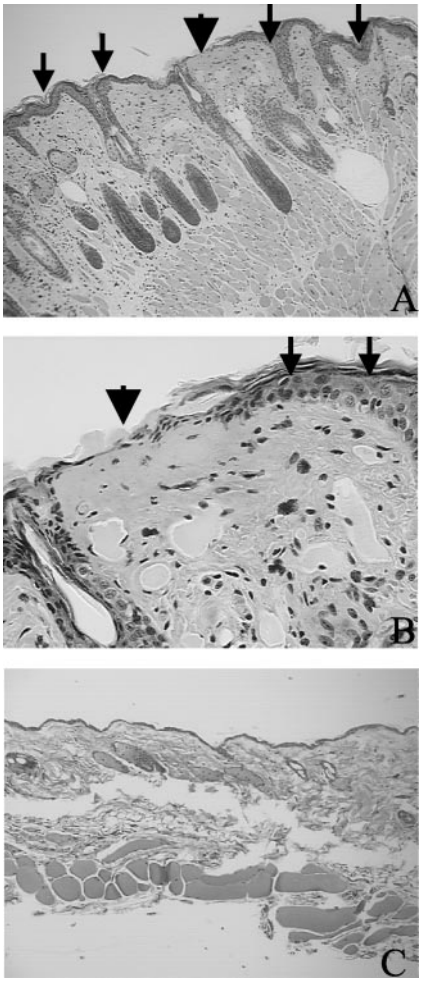

FIGURE 3. Histopathology of ventral cervical skin sections. *A* and *B*, Cervical skin from E$^{-/-}$P$^{-/-}$ mice was ulcerated (arrowhead) and showed a chronic hyperplastic epithelial response in areas bordering epithelial denudation (arrows). *A* and *B*, The dermis is characterized by a mixed inflammatory infiltrate, noticeably lacking in neutrophils but containing plasma cells, macrophages, and other mononuclear cells. *C*, Skin from E$^{-/-}$P$^{-/-}$Rag-1$^{-/-}$ mice showed none of the changes described in the E$^{-/-}$P$^{-/-}$ mice. The epithelium has a normal uniform thickness, and the dermis contains normal connective and muscular tissue with very few inflammatory cells present. Sebaceous glands and hair follicles also demonstrate normal architecture. Original magnification: *A* and *C*, ×10; *B*, ×40.

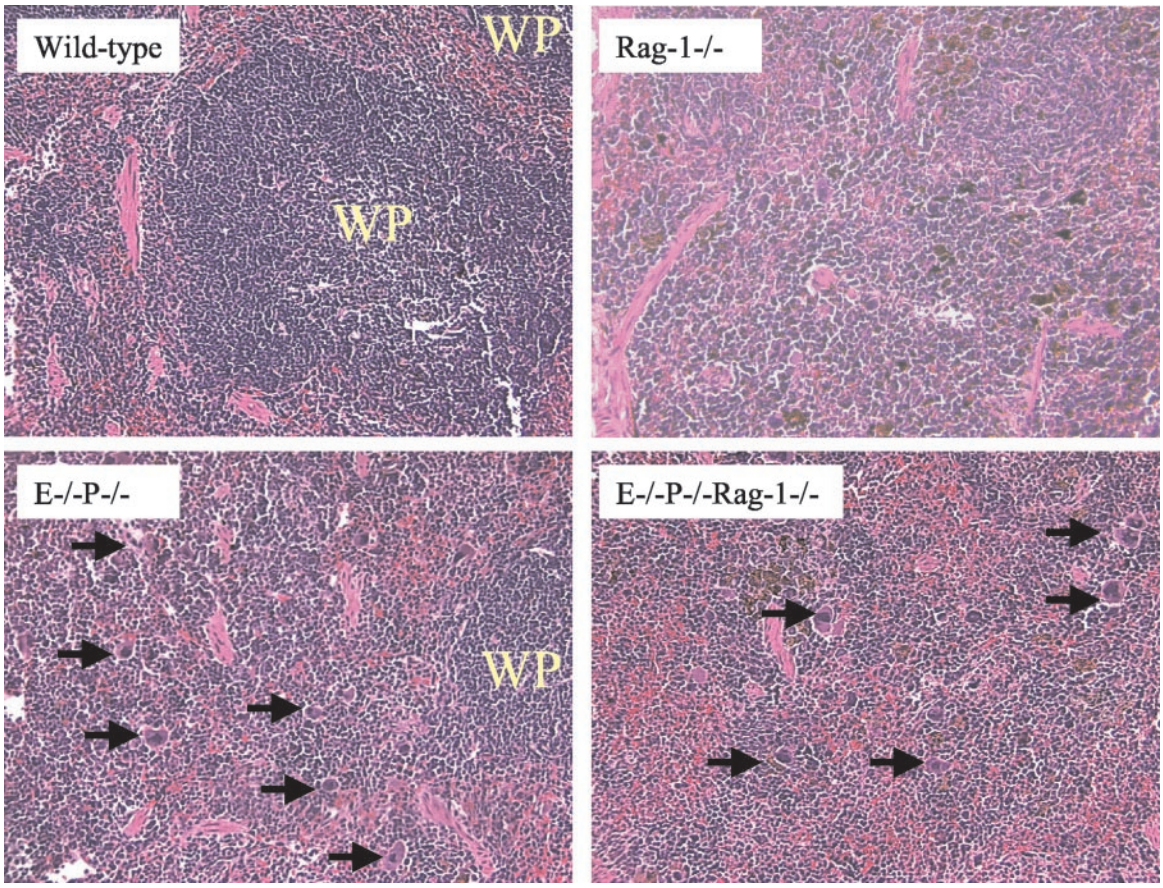

FIGURE 4. Histopathology of spleen sections. Rag-$1^{-/-}$ mice show a depletion of white pulp (WP) that is prominent in wild-type mice. Mice deficient in E- and P-selectin show distorted splenic architecture, including large numbers of neutrophils and expanded red pulp due to extramedullary hemopoiesis and smaller and distorted regions of WP with infiltration of plasma cells. $E^{-/-}P^{-/-}$Rag-$1^{-/-}$ mice also show extramedullary hemopoiesis; although these mice show an absence of WP. Arrows show increased presence of megakaryocytes, large myeloid, and erythoid precursors. Samples are from age-matched 8-mo-old mice. Original magnification: ×20.

Rag-1-deficient mice had small cervical lymph nodes (5.0 ± 0.4 mg) with few mature lymphoid cells (Fig. 6) compared with wild-type mice (11.0 ± 0.1 mg; Fig. 6; Table III). $E^{-/-}P^{-/-}$ mice displayed cervical lymphadenopathy (19.6 ± 2.4 mg), the normal corticomedullary architecture was disrupted, and lymph nodes were infiltrated by inflammatory mononuclear and plasma cells (Fig. 6). In some cases, particularly in mice with severe skin lesions overlying the submandibular lymph nodes, lymphoid follicles were completely effaced by plasma cells. $E^{-/-}P^{-/-}$Rag-$1^{-/-}$ mice had very small lymph nodes that were not different from Rag-1-deficient mice (3.7 ± 0.7 mg; Table III). These lymph nodes contained few lymphocytes, no plasma cell infiltrate, and more connective tissue and fibroblasts (Fig. 6). Colon, small intestine, liver, and kidney from all groups showed no significant pathology.

Discussion

The development of conjunctivitis and ulcerative dermatitis in $E^{-/-}P^{-/-}$ mice is associated with an active immune response and plasma cell infiltration of cervical lymph nodes. In this study, we show that $E^{-/-}P^{-/-}$Rag-$1^{-/-}$ mice lacking this immune response did not develop ulcerative dermatitis, showed small cervical lymph nodes, and decreased lung pathology compared with $E^{-/-}P^{-/-}$ mice. This indicates that an altered or enhanced immune response in $E^{-/-}P^{-/-}$ mice is, at least in part, causative of the phenotype.

Table III. *Spleen and lymph node weights*[a]

	Spleen wt[b] (mg)	Spleen wt/Body wt (mg/g)	One Cervical Lymph Node wt (mg)	Cervical Lymph Node wt/Body wt (mg/g)
Wild type	90 ± 6	3.0 ± 0.2[c]	11.0 ± 0.1[c]	0.36 ± 0.02[c]
Rag-$1^{-/-}$	62 ± 19[c]	2.3 ± 1.0[c]	5.0 ± 0.4[c]	0.18 ± 0.04[c]
$E^{-/-}P^{-/-}$	175 ± 21[d]	8.3 ± 1.2[c,e]	19.6 ± 2.4[d,e,f]	0.93 ± 0.09[d,e,f]
$E^{-/-}P^{-/-}$Rag-$1^{-/-}$	130 ± 20	5.0 ± 0.9	3.7 ± 0.7[c]	0.14 ± 0.03[c]

[a] All values expressed as mean ± SEM.
[b] wt, weight.
[c] Different from $E^{-/-}P^{-/-}$ group.
[d] Different from Rag-$1^{-/-}$ group.
[e] Different from wild-type group.
[f] Different from $E^{-/-}P^{-/-}$Rag-$1^{-/-}$ group ($p < 0.05$).

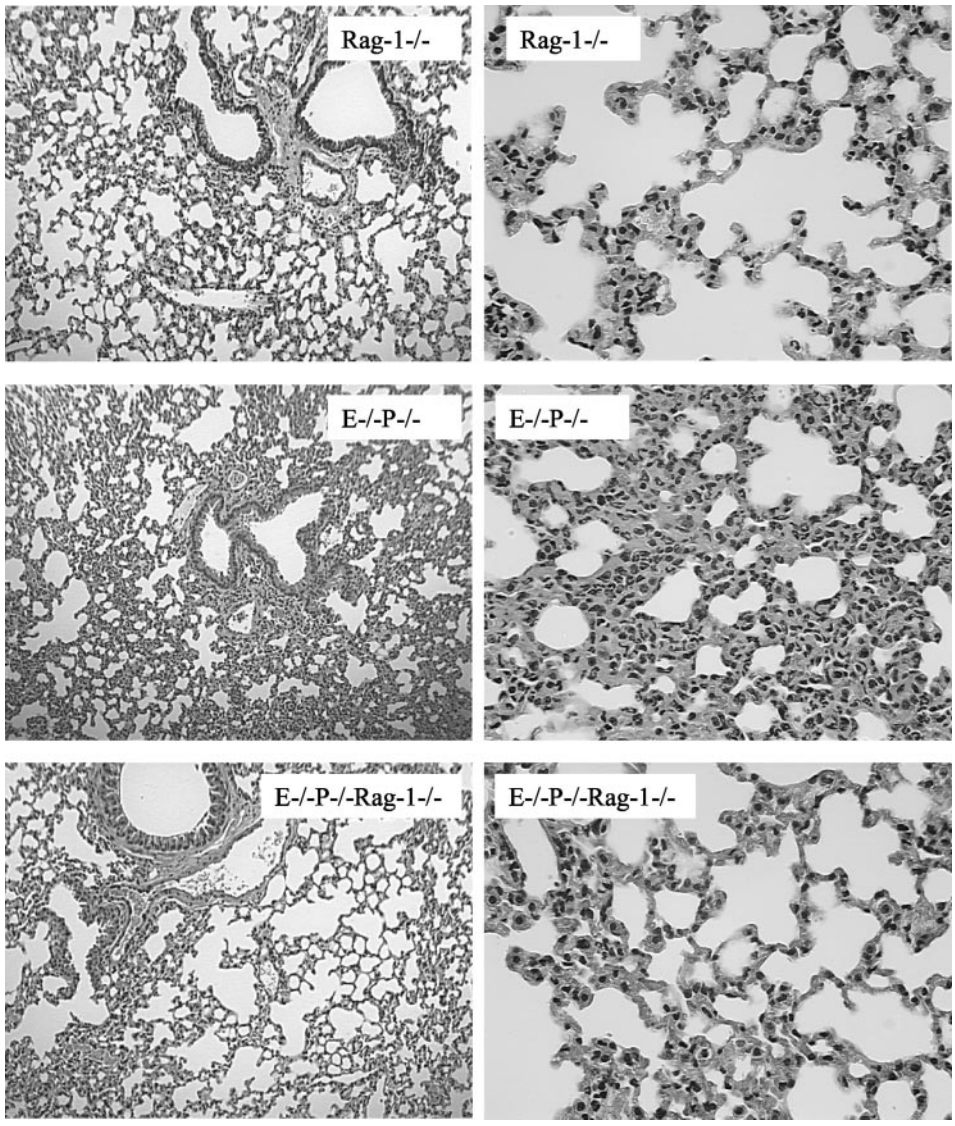

FIGURE 5. Histopathology of lung tissue. Lung sections from Rag-1$^{-/-}$ mice are not different from wild-type control mice (data not shown). E$^{-/-}$P$^{-/-}$ mice show mild to severe lung pathology. E$^{-/-}$P$^{-/-}$ mice showed significant neutrophil populations which appear to be both in the capillaries and the interstitial tissue diffusely throughout the entire lung. E$^{-/-}$P$^{-/-}$ mice with severe lung pathology also showed interstitial edema and hemorrhage. E$^{-/-}$P$^{-/-}$Rag-1$^{-/-}$ mice also showed high numbers of neutrophils in alveolar capillary beds and infiltrating interstitial regions, but much less severe than E$^{-/-}$P$^{-/-}$ mice. Leukocyte infiltrates in E$^{-/-}$P$^{-/-}$Rag-1$^{-/-}$ mice were more focal (*bottom left, left panel*) compared with the diffuse distribution in E$^{-/-}$P$^{-/-}$ mice. Samples are from age-matched 8-mo-old mice. Original magnification: *left panels*, ×10; *right panels*, ×40.

E$^{-/-}$P$^{-/-}$ mice develop ulcerative dermatitis of the nose and cervical regions at all institutions where they are bred. Mice lacking all three selectins (E$^{-/-}$P$^{-/-}$L$^{-/-}$) develop ulcerative dermatitis in some facilities (University of Washington, Seattle, WA; and Harvard Medical School, Boston, MA), while they are largely protected from disease development in other facilities (Baylor College of Medicine, Houston, TX; University of Virginia, Charlottesville, VA). The causative trigger of ulcerative dermatitis is not known but appears to be related to environmental and/or housing conditions. We hypothesized that the skin pathology results from a compensatory immune response to commensal bacteria, including plasma cell hyperproliferation, and that a diminished immune response in the absence of ICAM-1 (E$^{-/-}$P$^{-/-}$I$^{-/-}$) and L-selectin (E$^{-/-}$P$^{-/-}$L$^{-/-}$) protects these mice from disease development. In this study, we show that an absence of functional T and B cells (E$^{-/-}$P$^{-/-}$Rag-1$^{-/-}$) completely protects these mice from the development of ulcerative dermatitis, although housed in the same environment.

Histological analysis of skin sections of E$^{-/-}$P$^{-/-}$ mice reveals a complete absence of neutrophils in skin lesions, showing that neutrophils are not recruited to these areas of infection in the absence of E- and P-selectin. Interestingly, significant levels of lymphocyte recruitment occur despite the lack of E- and P-selectin. Lymphocyte recruitment to skin lesions is likely due to the critical involvement of α_4 integrins in the recruitment of lymphocytes to sites of chronic inflammation. We have shown that lymphocyte recruitment and adhesion were not affected in chronic models of inflammation (thioglycolate-induced peritonitis and 6-h TNF-α-induced inflammation of the mouse cremaster muscle, respectively) in mice lacking E-, P-, and L-selectin and ICAM-1 (E$^{-/-}$P$^{-/-}$L$^{-/-}$I$^{-/-}$; Ref. 15). Leukocyte adhesion was almost completely inhibited only with anti-α_4 integrin mAb pretreatment. T lymphocyte migration to dermal inflammation induced by IFN-γ, TNF-α, LPS, or poly inosine-cytosine was markedly reduced by anti-α_4 integrin treatment (50–60%). T lymphocyte migration was inhibited by only 30–60% with anti-E- and P-selectin treatment compared with 10–40% with either anti-E- or P-selectin treatment. Blockade of both E- and P-selectin and α_4 integrin function severely impaired lymphocyte recruitment in these models of dermal inflammation (>90%; Ref. 16). Although E- and P-selectin have a role in lymphocyte recruitment, they are not strictly required in some models of inflammation.

The molecular mechanisms linking a dysregulated immune response to conjunctivitis and cervical ulcerative dermatitis remain unknown and were not addressed in this study. Decreased neutrophil trafficking in E$^{-/-}$P$^{-/-}$ mice may result in expansion

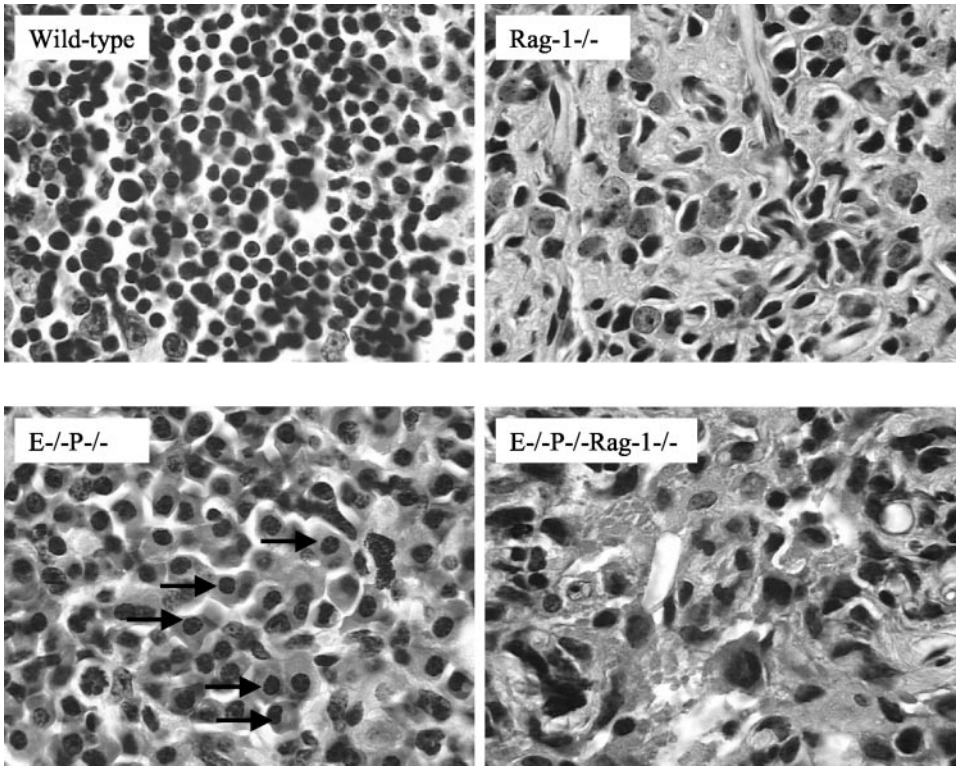

FIGURE 6. Histopathology of lymph node tissue. Cervical lymph nodes from $E^{-/-}P^{-/-}$ mice varied from moderate to severe inflammatory changes, characterized predominantly by replacement of normal lymphoid follicles with plasma cells (some shown by arrows), and some macrophages in the interstitium. $E^{-/-}P^{-/-}Rag^{-/-}$ lymph nodes were similar to $Rag^{-/-}$ mice in appearance, being grossly very small and composed primarily of fibroblasts, a few clusters of mononuclear cells around capillaries, and a mixed inflammatory cell infiltrate. Original magnification: ×100.

of commensal bacteria and an increased antigenic load which may lead to the release of proinflammatory cytokines which potentiate host tissue damage and ulceration. Others have shown that T cells are actively involved in inflammatory skin disorders, including allergic contact dermatitis, atopic dermatitis, and psoriasis (17–19). Cytokines released by activated skin infiltrating T lymphocytes, such as TNF-α, IFN-γ, and IL-4, induce the activation of keratinocytes to produce proinflammatory chemokines, including inducible protein-10, IFN-inducible T cell chemoattractant, and monokine induced by IFN-γ, which results in the continued recruitment of $CXCR^{3+}$ T cells (17). Chronic abnormal chemokine and proinflammatory cytokine production from activated infiltrating T cells and keratinocytes may lead to host tissue damage and lesion development. Consistent with this interpretation, removing lymphocyte function in $E^{-/-}P^{-/-}Rag\text{-}1^{-/-}$ mice eliminates this overshooting response to normal flora Ags and protects these mice from tissue damage and ulceration despite defective neutrophil trafficking. Remarkably, the same commensal bacteria colonizing dermal lesions in $E^{-/-}P^{-/-}$ mice do not invade $E^{-/-}P^{-/-}Rag\text{-}1^{-/-}$ mice. This suggests that the dysregulated immune response in $E^{-/-}P^{-/-}$ mice is pathogenic rather than protective under vivarium conditions.

Secretion of various cytokines from T cells promotes neutrophil recruitment and stimulates granulopoiesis, linking the acquired immune system with the innate system. IL-17 released from activated T cells has been shown to stimulate neutrophil recruitment through the release of keratinocyte-derived chemokine and macrophage-inflammatory protein-2 (20, 21). T cells regulate hemopoiesis through secretion of various cytokines, including IL-2, IL-3, IL-6, IL-8, IL-17, and GM-CSF (22, 23). IL-17 stimulates granulopoiesis in vivo through G-CSF release (22). $E^{-/-}P^{-/-}Rag\text{-}1^{-/-}$ mice show elevated serum G-CSF and levels of neutrophilia similar to $E^{-/-}P^{-/-}$ mice, suggesting that lymphocyte-independent mechanisms completely regulate the elevated neutrophil levels seen in these mice (~20,000 polymorphonuclear cells/μl). Surprisingly, $E^{-/-}P^{-/-}Rag\text{-}1^{-/-}$ mice do not show neutrophil levels higher than $E^{-/-}P^{-/-}$ mice. Although granulopoiesis can be enhanced or modulated by the acquired immune system (22), lymphocyte-independent granulopoiesis in $E^{-/-}P^{-/-}Rag\text{-}1^{-/-}$ mice is sufficient to compensate for the loss of the acquired immune system. This suggests there is an independence of the acquired and innate immune systems in regulating this level of neutrophilia.

In conclusion, we show that $E^{-/-}P^{-/-}Rag\text{-}1^{-/-}$ mice which lack functional lymphocytes display a healthier phenotype than $E^{-/-}P^{-/-}$ mice, although circulating neutrophil counts and serum G-CSF levels are similar to $E^{-/-}P^{-/-}$ mice. $E^{-/-}P^{-/-}Rag\text{-}1^{-/-}$ mice did not have hypercellular cervical lymph nodes and showed reduced leukocyte infiltrate in the lungs. Most importantly, $E^{-/-}P^{-/-}Rag\text{-}1^{-/-}$ mice were completely protected from the ulcerative dermatitis that develops in $E^{-/-}P^{-/-}$ mice. We conclude that a dysfunctional immune response in $E^{-/-}P^{-/-}$ mice resulting from impaired leukocyte trafficking leads to ulcerative dermatitis in $E^{-/-}P^{-/-}$ mice.

Acknowledgments

We thank Dr. Dan Bullard (University of Alabama, Birmingham, AL) for providing mice lacking E- and P-selectin, Dr. Marcie McDuffie (University of Virginia) for providing $Rag\text{-}1^{-/-}$ mice, Michele Kirkpatrick for animal husbandry, and the Research Histology Core (University of Virginia) for tissue processing services. We thank Dr. Geoff Kansas (Northwestern University, Evanston, IL) and Dr. Dan Bullard for valuable discussions that generated the project idea.

References

1. Bullard, D. C., E. J. Kunkel, H. Kubo, M. J. Hicks, I. Lorenzo, N. A. Doyle, C. M. Doerschuk, K. Ley, and A. L. Beaudet. 1996. Infectious susceptibility and severe deficiency of leukocyte rolling and recruitment in E-selectin and P-selectin double mutant mice. *J. Exp. Med. 183:2329.*
2. Jung, U., and K. Ley. 1999. Mice lacking two or all three selectins demonstrate overlapping and distinct functions for each selectin. *J. Immunol. 162:6755.*
3. Jung, U., C. L. Ramos, D. C. Bullard, and K. Ley. 1998. Gene-targeted mice reveal importance of L-selectin-dependent rolling for neutrophil adhesion. *Am. J. Physiol. 274:H1785.*
4. Frenette, P. S., T. N. Mayadas, H. Rayburn, R. O. Hynes, and D. D. Wagner. 1996. Susceptibility to infection and altered hematopoiesis in mice deficient in both P- and E-selectins. *Cell 84:563.*

5. Scharffetter-Kochanek, K., H. Lu, K. Norman, N. van Nood, F. Munoz, S. Grabbe, M. McArthur, I. Lorenzo, S. Kaplan, K. Ley, et al. 1998. Spontaneous skin ulceration and defective T cell function in CD18 null mice. *J. Exp. Med. 188:119.*
6. Frenette, P. S., C. Moyna, D. W. Hartwell, J. B. Lowe, R. O. Hynes, and D. D. Wagner. 1998. Platelet-endothelial interactions in inflamed mesenteric venules. *Blood 91:1318.*
7. Robinson, S. D., P. S. Frenette, H. Rayburn, M. Cummiskey, M. Ullman-Cullere, D. D. Wagner, and R. O. Hynes. 1999. Multiple, targeted deficiencies in selectins reveal a predominant role for P-selectin in leukocyte recruitment. *Proc. Natl. Acad. Sci. USA 96:11452.*
8. Collins, R. G., U. Jung, M. Ramirez, D. C. Bullard, M. J. Hicks, C. W. Smith, K. Ley, and A. L. Beaudet. 2001. Dermal and pulmonary inflammatory disease in E-selectin and P-selectin double-null mice is reduced in triple-selectin-null mice. *Blood 98:727.*
9. Mizgerd, J. P., D. C. Bullard, M. J. Hicks, A. L. Beaudet, and C. M. Doerschuk. 1999. Chronic inflammatory disease alters adhesion molecule requirements for acute neutrophil emigration in mouse skin. *J. Immunol. 162:5444.*
10. Arbones, M. L., D. C. Ord, K. Ley, H. Ratech, C. Maynard-Curry, G. Otten, D. J. Capon, and T. F. Tedder. 1994. Lymphocyte homing and leukocyte rolling and migration are impaired in L-selectin-deficient mice. *Immunity 1:247.*
11. Steeber, D. A., N. E. Green, S. Sato, and T. F. Tedder. 1996. Humoral immune responses in L-selectin-deficient mice. *J. Immunol. 157:4899.*
12. Xu, J., I. S. Grewal, G. P. Geba, and R. A. Flavell. 1996. Impaired primary T cell responses in L-selectin-deficient mice. *J. Exp. Med. 183:589.*
13. Sligh, J. E., C. M. Ballantyne, S. S. Rich, H. K. Hawkins, C. W. Smith, A. Bradley, and A. L. Beaudet. 1993. Inflammatory and immune responses are impaired in mice deficient in intercellular adhesion molecule 1. *Proc. Natl. Acad. Sci. USA 90:8529.*
14. Mombaerts, P., J. Iacomini, R. S. Johnson, K. Herrup, S. Tonegawa, and V. E. Papaioannou. 1992. RAG-1-deficient mice have no mature B and T lymphocytes. *Cell 68:869.*
15. Forlow, S. B., and K. Ley. 2001. Selectin-independent leukocyte rolling and adhesion in mice deficient in E-, P-, and L-selectin and ICAM-1. *Am. J. Physiol. 280:H634.*
16. Issekutz, A. C., and T. B. Issekutz. 2002. The role of E-selectin, P-selectin, and very late activation Ag-4 in T lymphocyte migration to dermal inflammation. *J. Immunol. 168:1934.*
17. Albanesi, C., C. Scarponi, S. Sebastiani, A. Cavani, M. Federici, O. De Pita, P. Puddu, and G. Girolomoni. 2000. IL-4 enhances keratinocyte expression of CXCR3 agonistic chemokines. *J. Immunol. 165:1395.*
18. Schuerwegh, A. J., L. S. De Clerck, L. De Schutter, C. H. Bridts, A. Verbruggen, and W. J. Stevens. 1999. Flow cytometric detection of type 1 (IL-2, IFN-γ) and type 2 (IL-4, IL-5) cytokines in T-helper and T-suppressor/cytotoxic cells in rheumatoid arthritis, allergic asthma and atopic dermatitis. *Cytokine 11:783.*
19. Giustizieri, M. L., F. Mascia, A. Frezzolini, O. De Pita, L. M. Chinni, A. Giannetti, G. Girolomoni, and S. Pastore. 2001. Keratinocytes from patients with atopic dermatitis and psoriasis show a distinct chemokine production profile in response to T cell-derived cytokines. *J. Allergy Clin. Immunol. 107:871.*
20. Laan, M., Z. H. Cui, H. Hoshino, J. Lotvall, M. Sjostrand, D. C. Gruenert, B. E. Skoogh, and A. Linden. 1999. Neutrophil recruitment by human IL-17 via C-X-C chemokine release in the airways. *J. Immunol. 162:2347.*
21. Witowski, J., K. Pawlaczyk, A. Breborowicz, A. Scheuren, M. Kuzlan-Pawlaczyk, J. Wisniewska, A. Polubinska, H. Friess, G. M. Gahl, U. Frei, and A. Jorres. 2000. IL-17 stimulates intraperitoneal neutrophil infiltration through the release of GROα chemokine from mesothelial cells. *J. Immunol. 165:5814.*
22. Schwarzenberger, P., V. La Russa, A. Miller, P. Ye, W. Huang, A. Zieske, S. Nelson, G. J. Bagby, D. Stoltz, R. L. Mynatt, et al. 1998. IL-17 stimulates granulopoiesis in mice: use of an alternate, novel gene therapy-derived method for in vivo evaluation of cytokines. *J. Immunol. 161:6383.*
23. Lord, B. I., C. M. Heyworth, and N. G. Testa. 1997. An introduction to primitive hematopoietic cells. In *Hematopoietic Lineages in Health and Disease*. N. G. Testa, B. I. Lord, and T. M. Dexter, eds. Marcel Dekker, New York, p. 1.